Magnetic Actuation and Localization of Sperm Based Micro-robots

J. R. Cumming

University of Twente, Faculty of Engineering Technology, Drienerlolaan 5, 7522 NB, Enschede, The Netherlands

ABSTRACT: Sperm cell based micro-robots may in the future be used for *in vivo* medical therapies such as targeted drug delivery. They can navigate small vessels and navigate parts of the body that are otherwise inaccessible. The aims of this study are two-fold. First, differential magnetometry as a method for magnetically localizing these micro-robots is evaluated. Second, a method for magnetically actuating nano-particle coated sperm clusters will be demonstrated. Micro-robots fabricated by coating sperm cells with super paramagnetic iron oxide nano-particles are used. It is shown that nano-particle coated sperm cells experience reduced performance compared to free nano-particles in suspension. This may introduce challenges for localization using differential magnetometry. The rolling velocity of clusters are measured and they are found to demonstrate unique behaviors dependent on an applied magnetic field. In the future, these methods may show broader application and development within medicine.

Key words: Micro-robots, nano-particles, magnetic detection, magnetic localization, sperm cells

1 INTRODUCTION

Micro-robots present the field of medicine with exciting new possibilities for delivering drugs and therapy to locations in the body currently inaccessible through conventional surgical methods. The small size of micro-robots allows for the potential navigation of narrow capillaries throughout the body and locations in the brain that are too narrow or too otherwise inaccessible to currently provide treatment[1].

Within the field of micro-robots, bio-hybrid designs are particularly promising. In nature cells and microorganisms show high energy conversion efficiency and robust locomotion that synthetic micro-robot designs have been unable to replicate[2]. Bio-hybrid micro-robot designs utilize a biological component such as dead cells in order to construct a robot that can most closely mimic the structures and locomotion patterns of living organisms[3].

Sperm cells present a unique opportunity for use as bio-hybrid micro-robots. They are through nature, uniquely designed for locomotion within the body. Dead sperm cells can be induced to tangle together and form clusters. Single sperm cell robots could be used to navigate narrow capillaries and larger clusters may be used for larger vessels. Sperm cells can also be coated with magnetic nano-particles. Then, using time varying magnetic fields, these clusters can be actuated and made to roll and controlled. This approach presents an opportunity to use sperm cells as micro-robots *in vivo*.

Recent research has demonstrated how single nano-particle coated sperm cells can be actuated and made to swim[4]. Limited research has also been done to characterize the rolling motion of sperm cells when subjected to rotating magnetic field and show how they can be loaded with drugs to potentially allow for targeted drug delivery. Rolling motion is particularly important for micro-robots because in comparison to actuating micro-robots with a pulling magnetic force, it can be done with a weaker magnetic field[5].

It is also necessary to track micro-robots, and magnetic localization is a promising method for doing so. In particular, differential magnetometry will be used as a method to localize sperm cell based micro-robots. This is a process that capitalizes on the non-linear magnetization of super-paramagnetic iron oxide nano-particles which will be used.

Differential magnetometry works by first subjecting a sample to an alternating magnetic field. The sample is consequently excited and it's magnetic susceptibility can be measured with a closely placed pickup coil. This may be done to measure nano-particles but noise will be generated by adjacent compounds and materials, in the case of *in vivo* detection, tissues[6].

In order to better detect small quantities of nano-particles and reduce interference from surrounding tissues, a varied static offset field is introduced. This is what defines differential magnetometry. Human tissues are diamagnetic and have a linear magnetization curve. By measuring the derivative of the magnetization of a sample under various offsets

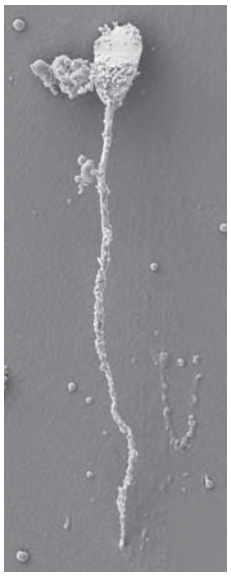

Fig. 1: A single sperm cell coated in nano-particles[8]

super-paramagnetic nano-particles can be differentiated from surrounding diamagnetic tissues or materials by their non-linear magnetization which contrasts the linear nature of surrounding tissue[6].

In this manner, differential magnetometry may allow relatively minuscule quantities of IRONSperm to be detected magnetically.

This study intends to firstly present a novel method for localizing nano-particle coated sperm cells using magnetic methods. Secondly, it will build on previous research done to investigate the rolling motion of sperm cells by looking at motion on a larger scale and characterizing the rolling motion of sperm cells based on magnetic field strength and rotational frequency

1.1 Sperm based micro-robots

Previous research has shown that by subjecting a sperm cell coated with magnetic nano-particles, here on defined as an IRONSperm, to a time varying magnetic field, the cells and their attached flagella can be made oscillate in such a way as to produce propulsion[7]. This presents an opportunity for navigation of narrow vessels within the body such as capillaries. Shown in Figure 1 is a single IRONSperm. A coating of nano-particles can be observed coating its flagellum and part of its head.

The specific nano-particles used to coat IRONSperm are super-paramagnetic iron oxide nano-particles(SPION). Synthetic iron oxide particles with a core size below 100 nm exhibit super-paramagnetic behavior. This means the particles exhibit a much greater magnetic susceptibility than bulk magnets. Additionally, when in the presence of a magnetic field they will become magnetized but upon removal of the field display no residual magnetic interaction[9]. The increased magnetic susceptibility of super-paramagnetic nano-particles allows IRONsperm to be magnetically actuated and localized with minimal quantities of iron present.

1.2 Fabrication of IRONsperm

IRONsperm is fabricated through a process in which dead bovine sperm cells are bound to super-paramagnetic iron oxide nano-particles through electrostatic interaction [4]. When a suspension containing sterilized bovine sperm cells is mixed with one of nano-particles and a charge is induced, an electrostatic attraction causes positively charged nano-particles and negatively charged sperm cells to bind to each other, causing nano-particles to form a surface coating on the sperm cells [4].

Two different varieties of nano-particle were used for the fabrication of IRONsperm. First, ellipsoid shaped nano-particles approximately 100 nm in major diameter were used. Synomag-70 nano-particles were used to fabricate a different sample of IRONsperm. Synomag-70 is a commercial variety of spherical nano-particle approximately 70nm in diameter.

The iron concentration of ellipsoid shaped nano-particles was 123 mg/ml in free suspension. The iron concentration and sperm concentration of IRONsperm fabricated with those particles was not determined.

The iron concentration of the Synomag-70 used to fabricate IRONSperm is known to be 25 mg/ml and the iron concentration of IRONSperm itself was determined to be 2.5 mg/ml. Additionally, the sperm concentration of this sample was determined to be 10e7 cells/ml

2 MAGNETIC LOCALIZATION

2.1 LapDiffMag

A laparoscopic differential magnetometer was used for the magnetic localization of sperm cells and nano-particles. It consists of an excitation coil, a probe, and

a control unit. The excitation coil is 27 cm in outer diameter and is used to simultaneously produce the static and alternating fields needed for detection[10].

The probe contains two coils used for detection [10]. They are encased at the end of a cylindrical rod 10 mm in diameter and 425 mm in length.

The control unit, placed on a wheeled trolley, contains the electronics needed for control, data processing and power amplification[10].

When a super-paramagnetic sample is placed within the excitation field and the detection probe is held in close proximity to a sample, a voltage is produced across the probe which is measured and recorded. The probe voltage is dependent on the distance from a sample.

During measurement, the probe needs to be held without any movement so a robotic arm was used to manipulate it with precision. Despite this, perfect alignment of the probe with respect to a sample is challenging and sub millimeter variations in alignment can have significant impacts on probe output voltage. For this reason, it is difficult to accurately repeat measurements performed with the LapDiffMag.

In order to perform a measurement with the LapDiffMag, the setup must first be calibrated without a sample present in order to obtain a reference. If the probe is to be measured at multiple points in space, calibration measurements must first be done at every point in space to be measured. Calibration is a time consuming process and because it must first be done without a sample present. After performing calibration, measurements may be performed. For accurate results a series of measurements is done and averaged. Each individual measurement takes approximately 1 second.

2.2 LapDiffMag Measurement Procedure

In order to characterize the voltage response of the probe as it is moved both horizontally and vertically with respect to a sample, two separate test procedures were designed.

The apparatus shown in Figure 2 was used to determine the probe voltage response as it is moved horizontally and vertically. The excitation coil is laid flat and a wooden block is placed at the center of the coil. The block has a hole bored into the center which is

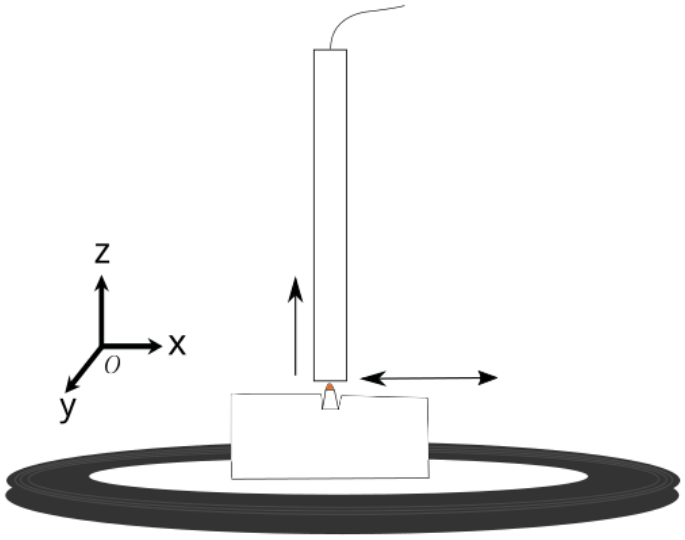

Fig. 2: Experimental setup for lateral probe measurements

used as a holder to fix a sample within the excitation field. Placed inside this holder is a 0.2 ml PCR tube which may hold volume of sample fluid. The PCR tube is placed top down within the holder such that the sample fluid is suspended through adhesion in the conical tip of the PCR tube at minimal distance from the probe tip.

The response to lateral and vertical movements was separately measured. To measure lateral response, the probe was suspended at a vertical distance of 0.5 mm, centered directly of the sample. It was then moved along the x-axis in 2 mm increments within the range -8 mm to 8 mm. At each point the average voltage of the probe over 10 measurements was recorded. To measure depth response, the probe was centered above the PCR tube with respect to the x and y axis. It was initially placed in contact with the top of the PCR tube at a distance of 0 mm from the sample and moved upward in 2 mm increments to a maximum range distance of 8 mm from the sample.

Lateral measurements were performed with both IRONsperm and nano-particles. Depth measurements were performed only with nano-particles.

2.3 Nano-particle measurements

The lateral test procedure was first repeated several times using a $50\,\mu L$ each quantity of Synomag-70 nano-particles with iron concentrations of 5 mg/ml, 15 mg/ml, and 25 mg/ml. The results are presented in Figure 3. Some initial measurements were performed

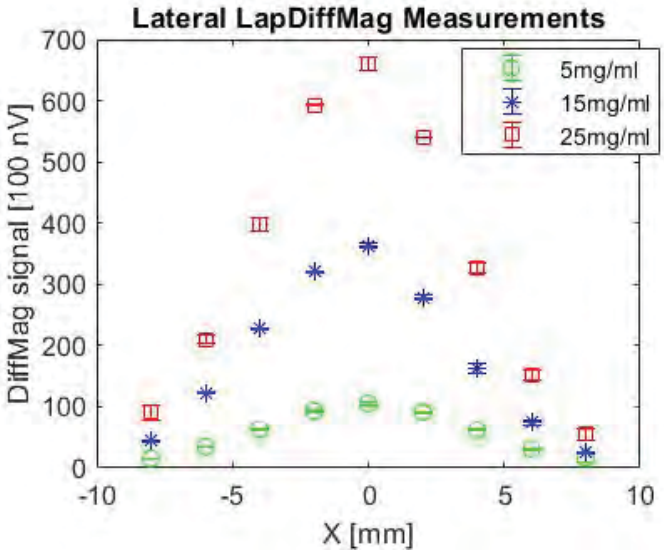

Fig. 3: Lateral probe measurements with three different concentrations of Synomag-70.

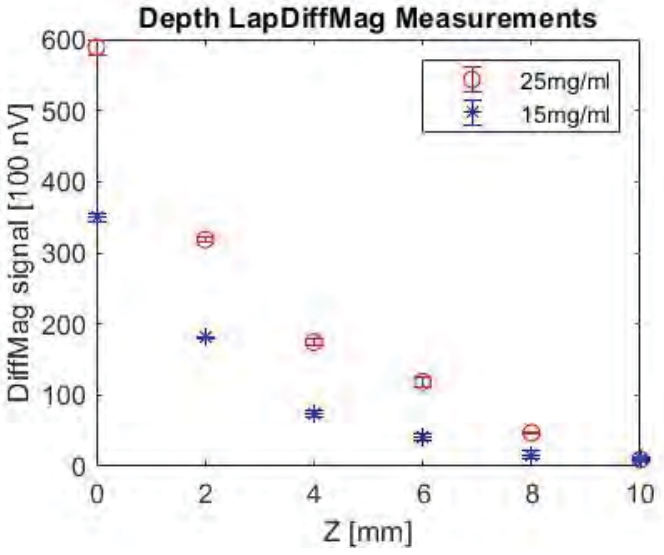

Fig. 4: The voltage decreases as the vertical distance between the probe and sample increases. Shown are measurements for two concentrations of Synomag-70 nano-particles.

with the ellipsoid shaped nano-particles. However, they produced a relatively weak response with the LapDiffMag and tests were not continued.

For all samples measured, the voltage of the probe decreased with distance from the sample. The voltage response was largely symmetric with the positive and negative x-axis. However, for samples with an iron concentration of 25 mg/ml and 15 mg/ml, negative values of x produced slightly greater voltages than corresponding positive values along the x-axis. It is expected that the voltage response should be symmetric as probe distance increases, and the observed behavior can likely be attributed to a to a misalignment of the probe when conducting these sets of measurements.

It was also observed that the probe voltage varied linearly with the iron concentration of a sample being observed. This behavior was expected based on previous research done with the LapDiffMag.

After performing lateral measurements, the depth test procedure was performed using $50\,\mu L$ samples of Synomag-70 with concentrations of 25 mg/ml and 15 mg/ml. Due to time constraints, a 5 mg/ml measurement could not be obtained. The results of the detection depth test are displayed in Figure 4.

For both samples measured, the probe voltage decreases as distance from the sample is increased. This is expected as the magnetic field generated by a magnet in a uniform magnetic field decays with the third power of distance[8]. Additionally by comparing measurements of multiple concentrations the voltage of the probe was further validated to be linearly proportional to iron concentration.

2.4 IRONSperm measurements

The experiments performed in the previous section were repeated using both varieties of IRONSperm discussed in Section 1.2. With both varieties of IRONSperm, no voltage above the background noise level was recorded.

The IRONSperm fabricated with ellipsoid shaped nano-particles was measured first using the lateral test procedure. A $100\,\mu L$ sample was initially used. Due to the suspected lack of their super-paramagnetic behavior, tests were not continued with the ellipsoid shaped particles.

Next, a lateral test was performed with a $100\,\mu L$ sample of IRONSperm fabricated with Synomag-70 nano-particles. Again no signal above the background noise level was detected. Based on the tests done with free Synomag-70 nano-particles it was expected that these IRONSperm would produce a response. A $100\,\mu L$ volume of IRONSperm with an iron density of 2.5 mg/ml would have the same iron quantity as the $50\,\mu L$ sample of free nano-particles shown in Figure 3 because its iron concentration is double that of the IRONSperm.

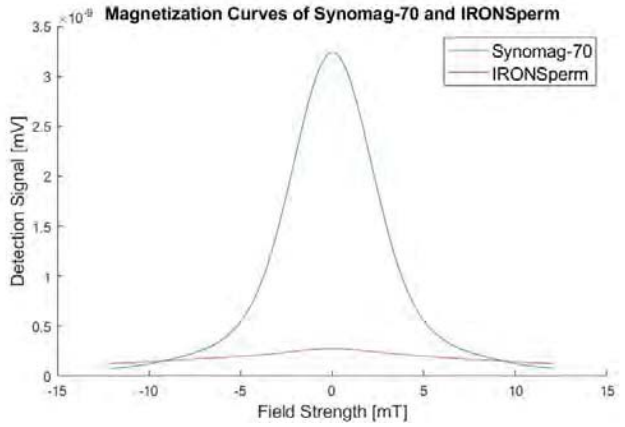

Fig. 5: Magnetization curves for Synomag-70 nano-particles and IRONSperm measured with the SPaQ.

A possible explanation for this behavior is that the magnetic susceptibility of nano-particles is reduced when they are bound to sperm cells. To quantify the reduction in magnetic susceptibility that occurred to nano-particles due to binding, additional tests were performed with a super-paramagnetic quantifier (SPaQ). This is a a more sensitive tabletop differential magnetometer specially designed for measuring the magnetization curve of super-paramagnetic nano-particles[11].

To compare nano-particles when they are free and when bound to IRONSperm, a $100\,\mu L$ sample of Synomag-70 IRONSperm was measured and compared to a $100\,\mu L$ sample of Synomag-70 free particles diluted to an iron concentration of 2.5 mg/ml. The iron content of both samples was equivalent. Both samples were individually measured with an excitation frequency of 500, 1000, 2500, and 5000 Hz. Excitation frequency did not significantly impact the response of the SPaQ. However, the most consistent magnetization response was produced at 1000 Hz and the results are shown in Figure 5

Figure 5 shows the magnetization curve of both samples at an excitation frequency of 1000 Hz. This can explain the poor performance of IRONSperm when measured with the LapDiffMag. The max signal difference of each curve ΔS_{max} is defined as its maximum measured amplitude subtracted by its minimum amplitude. This is a measure of a sample's measurement sensitivity[11]. The maximum signal difference of the measured Synomag-70 (3.16e-9 mV) sample was greater than that of the IRONSperm sample (1.50e-10 mV).

The full width of the curve at half maximum (FWHM) is another important property derived from the magnetization curve. It is used as a measure of the resolving power of a sample. The ratio of $\frac{\Delta S}{FWHM}$ is often used as a measure of sample's performance when measured using differential magnetometry[11].

Synomag-70 free particles had a $\frac{\Delta S}{FWHM}$ of (5.81e-10) compared to (1.49e-11) for IRONSperm, approximately 4 times greater. This likely explains why no signal was detected from IRONSperm when measured using the LapDiffMag.

Due to the decreased performance of IRONSperm with differential magnetometry, localization with the LapDiffMag is not feasible with the samples used. It may be possible to concentrate IRONSperm further and increase its iron concentration to compensate for reduced performance. Alternatively, a more sensitive differential magnetometer which can detect IRONSperm at low concentrations may be used.

2.5 Localization using LapDiffMag

Two procedures of magnetically localizing IRONSperm clusters using the LapDiffMag were considered. One possible option to localize IRONSperm with the LapDiffMag is to hold the probe position fixed and derive the position of an IRONSperm cluster relative to it based on the output probe voltage.

This method of localizing IRONSperm was initially considered. If the quantity and magnetization of IRONSperm is known, then it was originally believed that the voltage response of LapDiffMag could be analytically derived. In practice, the LapDiffMag does not have the necessary sensitivity to implement such a procedure and the system is too complex because the sample must be aligned with sub-millimeter precision using only visual feedback. It is consequently very difficult to control the position of the sample with respect all three axes. Additionally, the excitation field is non-uniform.[10] introduces additional complexity.

An alternative method of localization using the LapDiffMag is to perform a sweep along the axis of measurement, recording the probe voltage on a regular interval. If this is done, a pattern similar to the ones shown in Figure 3 will be observed. As the probe approaches the sample, the output voltage will increase. The location of a sample can then be identified by locating the maximum voltage during the sweep.

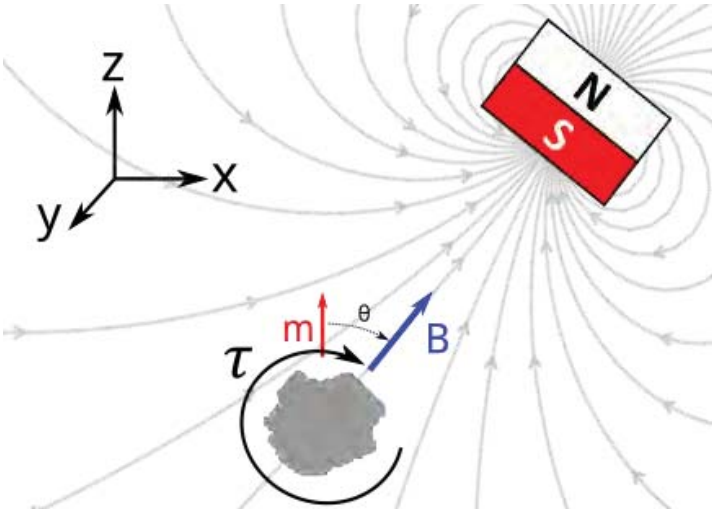

Fig. 6: Torque generated an IRONSperm

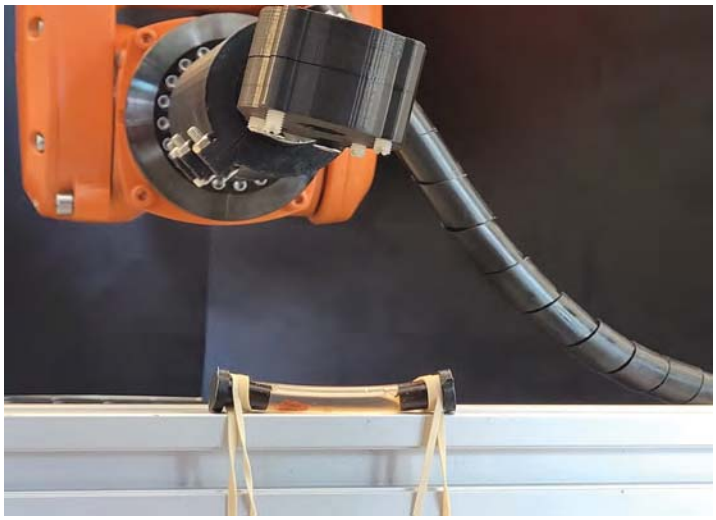

Fig. 7: The experimental actuation apparatus. A permanent magnet is held 75 mm above the IRONSperm in a plastic housing, exposing the IRONSperm to field of magnitude 6.2 mT.

Localizing IRONSperm using a sweep requires a set of multiple measurements to be done and will take significantly longer than the method in which position is derived using the theoretical model. However, this method is more robust because it does not rely on analytically determining the voltage-distance relation prior to measurement which was explained to be difficult. It is therefore recommended that a sweep be performed when localizing IRONSperm.

3 MAGNETIC ACTUATION

3.1 Theory of rolling magnetic actuation

Using a rotating magnetic field, IRONSperm clusters can be made to roll along a surface, producing motion. Clusters can also be actuated using a magnetic field, however the strength of a magnetic field needed to actuate clusters through magnetic attraction is much greater than the field needed to generate a comparable motion through rolling.

Consider the diagram displayed in Figure 6. An approximately spherical shaped IRONSperm cluster has been magnetized to a magnetic moment **m** within the presence of a magnetic field **B**.

The difference in alignment between the magnetic moment of the IRONSperm cluster and the magnetic field **B** can be described by the angle θ around the y axis. A magnetic torque τ will be inducted on the IRONSperm cluster described by Ampere's Law.

$$\tau = m \times B \quad (1)$$

When the IRONSperm are in contact with a surface, such as the bottom of a tube or vessel, this torque will produce a rolling motion and generate a translational movement parallel to the surface.

3.2 Experimental Procedure

To validate the theoretical model for magnetic actuation, an experimental apparatus was built with which IRONSperm was actuated. This is shown in Figure 7. An approximately $500\,\mu L$ sample of IRONSperm was diluted with $500\,\mu L$ of demineralized water and placed a plastic tube with a diameter of 6 mm and length of 37 mm. This tube was fixed to a square aluminum bar for stability.

Held above the IRONSperm filled tube was a permanent magnet whose rotational speed was controlled by a servo motor. The motor and permanent magnet were affixed to a 6-DOF KUKA robot which was used to position and control the height of the permanent magnet.

When placed in a magnetic field, individual IRONSperm clusters are subjected to a magnetic attractive force causing clusters to aggregate. This can be observed as IRONSperm pulled is out of suspension and collects into larger clusters on the bottom of the tube due to gravity.

To observe the rolling locomotion of IRONSperm, clusters were collected on one side of the plastic tube. The permanent magnet was then actuated with a angu-

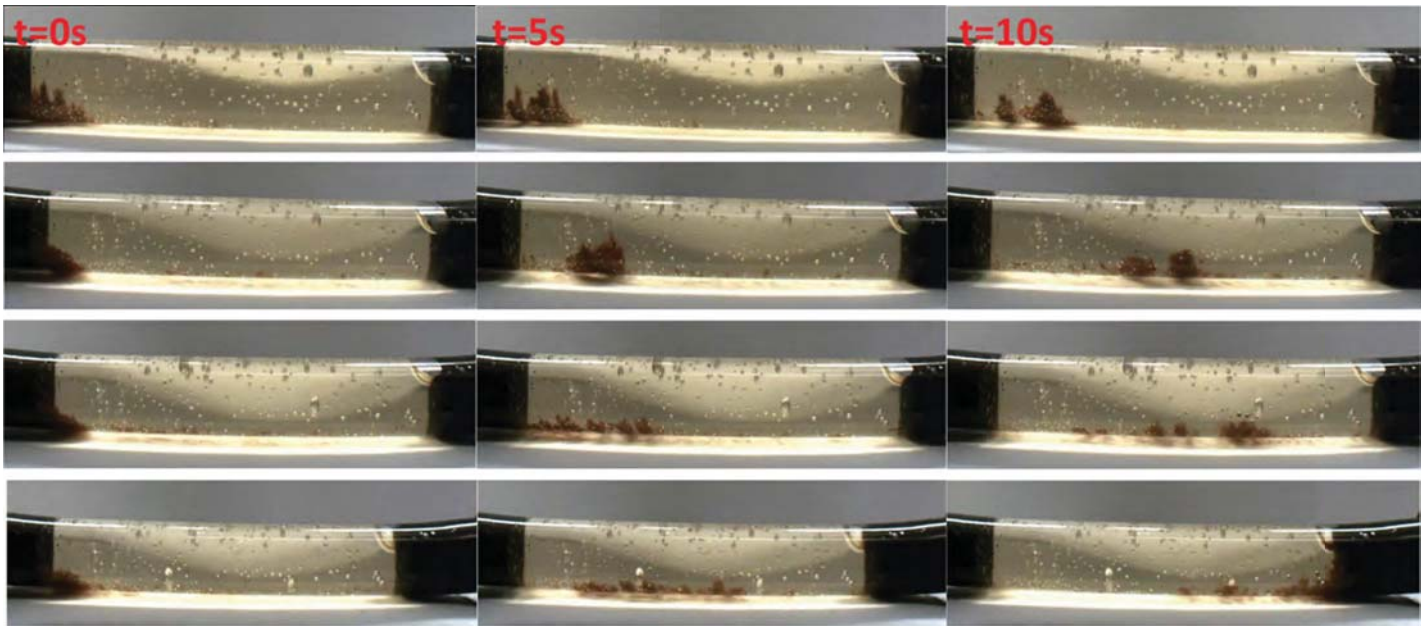

Fig. 8: Locomotion of IRONSperm under a rotating field of magnitude 6.2 mT. From top to bottom 5 RPM, 20 RPM, 60 RPM, and 140 RPM. Images are taken in 5 second intervals.

lar velocity to induce locomotion of the IRONSperm. Note that the permanent magnet was held centered above the plastic tube and was moved with the respect with the x, y or z-axis to produce locomotion.

This procedure was repeated using different rotational speeds of the permanent magnetic and varying its height above the tube to control the strength of the magnetic field which IRONSperm were subjected to.

3.3 Magnetic actuation results

Initially the permanent magnet was held above the IRONSperm tube. The resulting magnetic field was measured at the location of the tube and had a magnitude of 6.2 mT. The rolling motion and behavior of IRONSperm was then observed at a range of frequencies between 5 and 600 RPM. Snapshots of the measurements taken at 5, 20, 60, and 140 RPM are shown in Figure 8.

Under the rotating magnet field IRONSperm was observed aggregating into clusters and rolling along the bottom of the tube, their rotation in sync with that of the permanent magnet.

In Figure 8, a few unique behaviors of IRONSperm can be observed. At low frequencies such as 5 RPM and 20 RPM shown, large clusters tend to aggregate. At high frequencies significantly smaller clusters are observed forming.

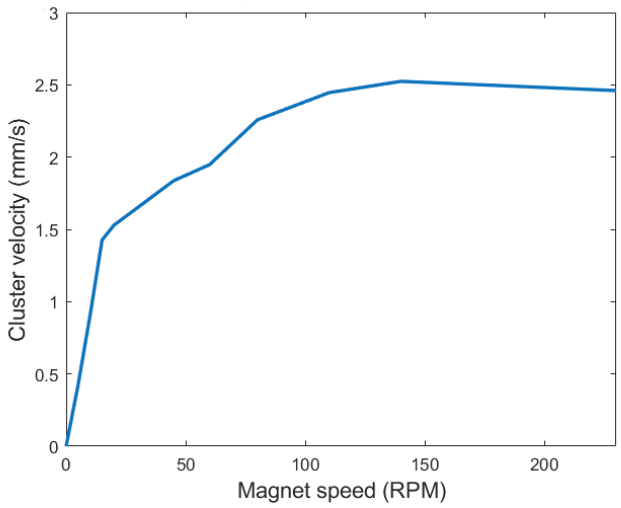

Fig. 9: Average rolling speed of IRONSperm under a magnetic field of magnitude 6.2 mT at various magnet RPMs.

A possible explanation for this behavior is that at high frequencies, clusters will surpass their step out frequencies and do not have time to align with the orientation of the rotating field. Because clusters may then rotate at different frequencies, they will have difficulty aggregating. Additionally, the bonds between individual clusters are relatively fragile and high accelerations may cause larger more fragile clusters to collapse into smaller ones.

Figure 9 shows the average rolling speed of clusters

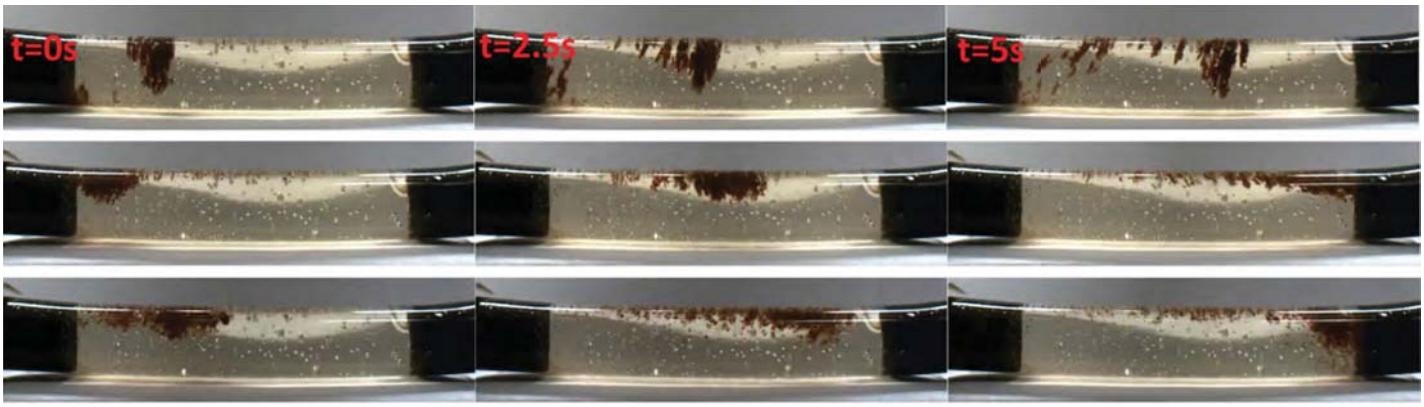

Fig. 10: Locomotion of IRONSperm under a rotating field of magnitude 9.32 mT. From top to bottom 20 RPM, 140 RPM, and 280 RPM counterclockwise. Images are taken in 2.5 second intervals.

at various magnet rotation speeds. It was observed that IRONSperm clusters move faster at higher rotation speeds of the permanent magnet. Up until a magnet speed of 25 RPM, the relation between cluster velocity and magnet speed was approximately linear. Cluster velocity then started to taper of and showed a slight decrease past 140 RPM. The linear relation at low RPMs may be explained by large rotating in sync with the permanent magnet and showing a proportional increase in velocity. The taper may be explained by small clusters beginning to form at intermediate RPMs, and although they may be rotating in sync with the magnet, due to their smaller diameter, these clusters experienced a lower velocity. Past 140 RPM, clusters may have begun to step out and as a consequence, experience reduced rotational velocity. Note that is graph was plotted with relatively few data points and more data should be collected to validate these results.

The strength of the magnetic field to which a clusters are subjected plays a significant role in their rolling behavior. Rolling motion was observed in IRONSperm under magnetic field strengths as low as 1.8 mT, although their speed was greatly reduced. Unique behavior was observed when the magnetic field strength was increased by lowering the height of the magnet. At a field strength of approximately 8.8 mT, the attractive forces between IRONSperm clusters and the permanent magnet were sufficiently large to pull clusters against the top wall of the tube overcoming gravity. To observe rolling behavior along the top of the tube, additional measurements were performed under a field strength of 9.3 mT. Snapshots of these are displayed in Figure 10. Note that the time interval of snapshots in Figure 10 is half that of 8 due to increased rolling speed of clusters.

Under a field strength of 9.3 mT measurements were performed by varying the rotational speed of the magnet at 20, 140, and 280 RPM in the counterclockwise direction. When IRONSperm clusters are in contact with the top of the tube, they were observed to roll counter to the rotation of the permanent magnet.

It was also observed under a stronger magnetic field and rolling along the top surface of the tube, clusters were able to achieve a greater rolling velocity. It is apparent from comparing the 20 RPM and 140 RPM in Figures 8 and 10, that under an increased magnetic field yet equal rotational speed of the magnet, clusters achieve a higher rolling frequency.

Furthermore, under a stronger magnetic field, clusters exhibit an increased step-out frequency. Under a field strength of 6.2 mT, cluster speed did not increase past magnet speeds of 140 RPM. Seen in Figure 10, an increase in cluster velocity is observed between magnet speeds of 140 RPM and 280 RPM counterclockwise . This can be explained by Equation 1. The torque that is applied to a cluster is directly proportional to the magnetic field **B**. Because a higher torque is applied under a greater magnetic field, the step-out frequency of clusters is increased.

4 CONCLUSIONS

In this study, methods for magnetically actuating and localizing nano-particle coated sperm cells were explored. To localize IRONSperm differential magnetometry was considered due to its ability to detect the

super-paramagnetic nano-particle coating of IRONSperm. It was observed that nano-particles experienced a reduction in magnetic susceptibility and detection performance through the process of binding to sperm cells when compared to particles in free suspension. As a consequence, localization of IRONSperm was not achieved using the LapDiffMag differential magnetometer.

Also in this study, IRONSperm clusters were actuated using a rotating field generated by a permanent magnet held above a fluid filled tube containing IRONSperm. Cluster velocity was observed to increase with both the rotational velocity of the permanent magnet as well as the magnitude of the applied magnetic field. Additional behavior was also observed. IRONSperm cluster size was dependent on magnet rotation frequency and under a sufficiently strong magnetic field, a pulling magnetic force between clusters and the permanent magnet was observed. Clusters were pulled against the top wall of the tube and rolled counter to the rotation of the permanent magnet.

Sperm based micro-robots are a viable future method for targeted drug delivery and other forms of therapy. Magnetic localization using differential magnetometry may allow the tracking of minimal amounts of these robots *in vivo*. Using low strength and rotating magnetic fields to actuate sperm through rolling, it may also be possible to navigate these robots to very specific and currently unreachable sites within the body. The combined application of these technologies will allow for greatly improved care within the field of medicine.

ACKNOWLEDGEMENTS

I would foremost like to express my deepest gratitude to my primary supervisor I. S.M. Khalil for his continuous guidance and support which made this work possible. I would additionally like to thank S. Salamzadeh and S. Tesselaar for their guidance and patience in assisting me with using the SPaQ and LapDiffMag systems. Lastly, I would like to thank L. Alic for her revision and insight regarding the localization of IRONSperm.

REFERENCES

[1] B. Nelson, I. Kaliakatsos, and J. Abbott. “Microrobots for Minimally Invasive Medicine”. In: *Annual Review of Biomedical Engineering* (2010).

[2] Z. Lin, T. Jiang, and J. Shang. “The emerging technology of biohybrid micro-robots: a review”. In: *Bio-Design and Manufacturing* (2021).

[3] Y. Moriomoto, H. Onoe, and S. Takeuchi. “Biohybrid robot with skeletal muscle tissue covered with a collagen structure for moving in air”. In: *APL Bioengineering* (2020).

[4] V. Magdanz et al. “IRONSperm: Sperm-templated soft magnetic microrobots”. In: *Science Advances* (2020).

[5] K. Middelhoek et al. “Drug-Loaded IRONSperm Clusters: Modeling, Wireless Actuation, and Ultrasound Imaging”. Unpublished. 2022.

[6] S. Waanders et al. “A handheld SPIO-based sentinel lymph node mapping device using differential magnetometry”. In: *Phys. Med. Biol.* (2016).

[7] J. Dias et al. “Modeling and Characterization of the Passive Bending Stiffness of Nanoparticle-Coated Sperm Cells using Magnetic Excitation”. In: *Advanced Theory and Simulations* (2022).

[8] I. S.M. Khalil, A. Klingner, and S. Misra. *Mathematical Modeling of Swimming Soft Microrobots*. Academic Press, 2021.

[9] S. Arora. “Superparamagnetic iron oxide nanoparticles: magnetic nanoplatforms as drug carriers”. In: *International Journal of Nanomedicine* (2012).

[10] M. Loosdrecht et al. “Laparoscopic Probe for Sentinel Lymph Node Harvesting Using Magnetic Nanoparticles”. In: *IEEE Transactions on Biomedical Engineering* (2022).

[11] M. M. Horstman et al. “Improving detection of magnetic nanoparticles: assessing excitation field frequency by SPaQ”. ”Unplublished”.